Simultaneous Detection of Liquid Level and Refractive Index with a Long Period Fiber Grating Based Sensor Device

Ying Huang[1], Baokai Chen[2], Genda Chen[3], Hai Xiao[2], and Samee U Khan[4]

[1]Department of Civil Engineering, North Dakota State University, Fargo, ND, 58108, U.S.A

[2]Department of Electrical and Computer Engineering, Missouri University of Science and Technology, Rolla, MO, 65409, U.S.A

[3]Department of Civil, Architectural, and Environmental Engineering, Missouri University of Science and Technology, Rolla, MO, 65409, U.S.A

[4]Department of Electrical and Computer Engineering, North Dakota State University, Fargo, ND, 58108, U.S.A

ying.huang@ndsu.edu and gchen@mst.edu

Abstract In this study, a long-period fiber grating (LPFG) based optical fiber sensor device is proposed for simultaneous detection of liquid level and refractive index. When part of the grating was submerged in an unknown liquid, the resonant wavelength of each cladding mode of the LPFG sensor varied linearly with the submerged length and nonlinearly with the refractive index of the liquid. By retaining the first-order (sensitivity) and second-order (cross sensitivity) terms of a Taylor expansion of the nonlinear relation, the changes in submerged length (or liquid level) and refractive index can be simultaneously evaluated from the changes in resonant wavelength of two cladding modes. The sensitivity coefficients to liquid level, refractive index, their cross effect, and environmental effects were studied both analytically and experimentally. The maximum prediction error by the proposed evaluation algorithm was found to be 1 mm for liquid level and 0.005 for refractive index.

Keywords Long-period fiber grating, Liquid level, Refractive index, Multiple parameter sensing

1. INTRODUCTION

An accurate assessment of both the level and type of liquid is critical in many applications such as water resources, environmental engineering, flood monitoring, and chemical processing and storage. Due to high sensitivity to environmental factors, long-period fiber grating (LPFG) sensors have been individually investigated for the measurement of refractive index and liquid level since the first successful fabrication in 1996 [1~3].

The resonant wavelength of LPFGs is a strong function of the change in its surrounding refractive index, which forms the basis of LPFG sensing. Thus, LPFGs is principally a refractive index (RI) sensor and, as such, has attracted wide attention from the research community since the invention of LPFG sensors. For example, the resonant peak changes of LPFGs induced by a change of ambient RI were first investigated in 1997 [4] and in 1998 [5]. The sensitivity of LPFG sensors for RI detection was further studied for the conditions of environmental RI lower [6] or higher than the effective RI of fiber cladding [7, 8]. To improve the sensitivity of LPFG refractors, various LPFG fabrication processes were studied, including Ultraviolet (UV light) [1~8], mechanically [9], and CO_2 laser [10], femtosecond laser [11] induced LPFGs. In addition, random-hole fibers modified from single-mode fibers were introduced [12]. To minimize or eliminate the nonlinear response of LPFG refractors, which limits their wide applications, special designs of LPFGs with linear response using experimental and theoretic generic algorithms were investigated [13, 14]. With their enhanced RI sensitivity, LPFG-based devices for chemical concentration measurements were developed [15, 16]. The previous research studies demonstrated that LPFG sensors possess high sensitivity and accuracy for environmental RI detection.

High RI-sensitivity LPFG sensors were also applied for liquid level measurements when partially submerged in particular liquids. For example, a potential use of LPFG sensors for oil level detection was demonstrated in 2001 [17]. Their experiments indicated a large linear range of the wavelength-level relation with a high sensitivity of 4.8% wavelength change per millimeter change in oil level. Liquid level detection was also reported with a 100 mm-long grating sensor in 2009 [18], a regular LPFG sensor in 2012 [19], and an LPFG modified Mach–Zehnder Interferometer in 2011 [20]. These advances of LPFG

liquid level sensors further led to the development of reflective LPFG series for simultaneous fluid level and velocity detection [21].

However, to date, LPFG sensors have not yet been applied for a simultaneous detection of liquid level and type (environmental RI) like fiber Bragg grating sensors and plastic fiber sensors [22, 23]. In this study, an LPFG- based optical fiber sensor device is proposed and developed for the measurement of both liquid level and refractive index. The device consists of two parallel LPFGs and one glass tube. One LPFG is installed outside the glass tube with two ends bonded on the glass tube and the other LPFG is installed in parallel inside the glass tube with two ends of the glass tube sealed. The LPFG outside the glass tube is the main sensing component for a simultaneous measurement of liquid level and surrounding RI; the one inside the glass tube is for temperature and pressure compensations. The LPFGs used in this paper are fabricated with CO_2-laser irradiation. Two cladding modes of an LPFG sensor, e.g. LP_{06} and LP_{07}, were used to relate the liquid level and environmental RI to the change in resonant wavelengths of the LPFG sensor. A simple algorithm for simultaneous determination of the liquid level and environmental RI (then type of the liquid) was analytically formulated and experimentally validated.

2. PRINCIPLES OF OPERATION

LPFGs with periodical changes along an optical fiber can couple the light propagating in the fiber core to various forward propagating cladding modes. Due to high optical loss of the cladding modes, a number of distinctive resonant valleys can be identified in the transmission spectrum of a typical LPFG sensor. The LPFGs used in this study were fabricated with a CO_2 laser irradiation technique [24]. The resonant wavelength ($\lambda_{res,m}$) of the m^{th} cladding mode (LP_{0m}) of an LPFG is proportional to its grating period (Λ) and the difference in effective refractive index, $\Delta n_{eff,m}$, between the core mode ($n_{eff,co}$) and the cladding mode LP_{0m} ($n_{eff,cl,m}$) [25]:

$$\lambda_{res,m} = \Delta n_{eff,m} \Lambda \tag{1}$$

For a given LPFG sensor, the grating period is known and the effective refractive index of the core ($n_{eff,co}$) changes little with the RI of surrounding medium. However, the effective refractive index of the

cladding mode ($n_{eff,cl,m}$) is significantly affected by the environmental RI. As a result, when partially immerged in a liquid, the coupling of light of an LPFG sensor from core to cladding strongly depends upon the fraction of the gratings submerged into the liquid (liquid level) and the liquid type (RI). Similar to simultaneous strain and temperature measurements [26], both $\Delta n_{eff,m}$ and Λ can be considered as two analytic functions of liquid level (L_{liquid}) and RI (n_s). Thus, Eq. (1) can be expanded into a Taylor series at the initial surrounding refractive index (n_0) and the complete submersion of all gratings (grating length L) as follows:

$$d\lambda_{res,m} = dn_s \cdot \left.\frac{\partial \lambda_{res,m}}{\partial n_s}\right|_{n_0,L} + dL_{liquid} \cdot \left.\frac{\partial \lambda_{res,m}}{\partial L_{liquid}}\right|_{n_0,L} + dn_s dL_{liquid} \cdot \left.\frac{\partial^2 \lambda_{res,m}}{\partial n_s \partial L_{liquid}}\right|_{n_0,L} + \frac{1}{2}[(dn_s)^2 \left.\frac{\partial^2 \lambda_{res,m}}{\partial^2 n_s}\right|_{n_0,L} + (dL_{liquid})^2 \left.\frac{\partial^2 \lambda_{res,m}}{\partial^2 L_{liquid}}\right|_{n_0,L}] + \ldots \tag{2}$$

where $\left.\frac{\partial \lambda_{res,m}}{\partial n_s}\right|_{n_0,L}$ and $\left.\frac{\partial \lambda_{res,m}}{\partial L_{liquid}}\right|_{n_0,L}$ respectively denote the sensor sensitivity to the surrounding refractive index and to the liquid level at $n_s = n_0$ and L_{liquid} = L; $\left.\frac{\partial^2 \lambda_{res,m}}{\partial n_s \partial L_{liquid}}\right|_{n_0,L}$ is the cross sensitivity effect between the surrounding refractive index and the liquid level, which can be evaluated by the sensor sensitivity to the liquid level in various types of liquid or different refractive indices. When the surrounding refractive index and liquid level are slightly changed, e.g. dn_s and dL_{liquid}, the high-order terms in Eq. (2) are negligible. As such, the first few terms can be used to approximate the change in LPFG resonant wavelength [27, 28] and Eq. (2) can be simplified into [26]:

$$d\lambda_{res,m} = dn_s \cdot \left.\frac{\partial \lambda_{res,m}}{\partial n_s}\right|_{n_0,L} + dL_{liquid} \cdot \left.\frac{\partial \lambda_{res,m}}{\partial L_{liquid}}\right|_{n_0,L} + dn_s dL_{liquid} \cdot \left.\frac{\partial^2 \lambda_{res,m}}{\partial n_s \partial L_{liquid}}\right|_{n_0,L} \tag{3}$$

Specifically, Eq. (3) includes the first-order RI change induced effect, first-order liquid level change induced effect, and the second-order cross-sensitivity between RI and liquid level.

2.1 Sensitivity to Surrounding Refractive Index

When the gratings are fully submerged into the liquid, the sensitivity of the gratings to the

surrounding refractive index can be written as [29]:

$$\frac{\partial \lambda_{res,m}}{\partial n_s} = \lambda_{res,m} \cdot K_{n_s,m} \tag{4}$$

where the dependence of the gratings on the surrounding refractive index ($K_{n_s,m}$) for cladding mode LP_{0m} can be evaluated by [29]:

$$K_{n_s,m} = -\gamma_m \cdot \frac{u_m^2 \lambda_{res,m}^3 n_s}{8\pi r_{cl}^3 n_{cl} \Delta n_{eff} \left(n_{cl}^2 - n_s^2\right)^{\frac{3}{2}}} \tag{5}$$

in which γ_m describes the waveguide dispersion for cladding mode LP_{0m}, which is positive for lower cladding modes and negative for higher cladding modes with a sign change point as a function of the resonant wavelength range [29]; u_m is the m^{th} root of the $zero^{th}$-order Bessel function of the first kind, r_{cl} is the radius of the cladding; and n_{cl} is the RI of the cladding. It can be clearly seen from Eq. (5) that $K_{n,m}$ is a nonlinear function of the resonant wavelength and the surrounding RIs. Previous researches showed that CO_2 laser induced LPFGs change the sign of their waveguide dispersion around 10^{th} mode for RI sensing [30]. As such, when the cladding mode is lower than 10^{th} mode, $K_{n,m}$ remains negative in almost all application cases, leading to a downshift of resonant wavelength of the grating as the liquid RI increases [31]. The higher the order of a cladding mode, the more sensitive the mode is to surrounding RI [29].

To simplify the process of determining multiple parameters (e.g. liquid level and surrounding RI), piecewise linear approximation is applied to linearize $K_{n,m}$ in various ranges of the surrounding RI using optimized data points obtained following the published procedure [32].

2.2 Sensitivity to Liquid Level

With a given surrounding refractive index, the resonant wavelength of an LPFG sensor can be calculated as a function of the full width at half maximum (FWHM) of the spectral resonance ($\lambda_{FWHM,m}$) for cladding mode LP_{0m}, the difference between effective refractive indices of the core and cladding modes ($n_{eff,co}$, $n_{eff,cl,m}$), and the length (L) of the LPFG [2]. That is,

$$\lambda_{res,m}{}^2 = 0.8\lambda_{FWHM,m} L \Delta n_{eff,m} \tag{6}$$

When LPFGs are partially submerged into the liquid by L_{liquid} in length and the other part remains in air, the resonant wavelengths of two fractions of the gratings in liquid and air can be expressed into:

$$\begin{cases} \lambda_{res,m,liquid}{}^2 = 0.8\lambda_{FWHM,m} L_{liquid} \Delta n_{eff,m,liquid} \\ \lambda_{res,m,air}{}^2 = 0.8\lambda_{FWHM,m} (L - L_{liquid}) \Delta n_{eff,m,air} \end{cases} \tag{7}$$

In the derivation of Eq. (7), the total grating length ($L = L_{air} + L_{liquid}$) was divided into the dry portion in air (L_{air}) and the wet portion in liquid (L_{liquid}); $\Delta n_{eff,cl,m,air}$ and $\Delta n_{eff,cl,m,liquid}$ represent the differences between the effective refractive indices of fiber core and cladding in air and liquid, respectively. The resultant resonant wavelength (in square) of the immersed LPFGs in liquid is then defined as an average of the difference between the two fractions with different surrounding RIs:

$$\lambda_{res,m}{}^2 = 0.4\lambda_{FWHM,m} \left[L\Delta n_{eff,m,air} + L_{liquid} (\Delta n_{eff,m,liqid} - \Delta n_{eff,m,air}) \right] \tag{8}$$

As a result, sensitivity of the LPFG sensor to the liquid level can be written as:

$$\frac{\partial \lambda_{res,m}}{\partial L_{liquid}} = \lambda_{res,m} K_{L_{liquid,m}} \tag{9}$$

where $K_{L_{liquid,m}}$ represents the dependence of grating over the length that is submerged into the liquid and can be derived into Eq. (10) by taking partial directive of Eq. (8) with respect to L_{liquid}:

$$K_{L_{liquid,m}} = 0.2 \frac{\lambda_{FWHM,m}}{\lambda_{res,m}} \left(\Delta n_{eff,m,liquid} - \Delta n_{eff,m,air} \right) \tag{10}$$

It can be seen from Eq. (10) that within the grating length, $K_{Liquid,,m}$ approximately changes linearly with the surrounding refractive index (represented by the type of liquid) provided that $\lambda_{FWHM,m}$ remains constant as the liquid level changes. When the refractive index of the liquid is less than that of the fiber cladding ($n_{cl} = 1.45$) and the highest cladding mode of the LPFG is less than 10th order [30], $\Delta n_{eff,cl,m,air} > \Delta n_{eff,cl,m,liquid}$ and a negative grating sensitivity to liquid level is achieved with downshifting resonant wavelength as the liquid level rises [31]. The higher the cladding mode, the more sensitive the grating is to liquid level [30]. In this study, the RI of target liquids for detection is bounded by those of water and fiber cladding (1.33 for water < n_s <1.45 for fiber cladding).

2.3 Cross-sensitivity Analysis

By taking derivative of Eq. (9) with respect to n_s and introducing Eq. (4), the cross sensitivity effect or the last term of Eq. (3) can be expressed into:

$$\frac{\partial^2 \lambda_{res,m}}{\partial n_s \partial L_{liquid}} = \frac{\partial\left(\frac{\partial \lambda_{res,m}}{\partial L_{liquid}}\right)}{\partial n_s} = \lambda_{res,m}(K_{n_s,m} K_{L_{liquid},m} + \frac{\partial K_{L_{liquid},m}}{\partial n_s}) \tag{11}$$

2.4 Simultaneous Detection of Liquid Level and Surrounding Refractive Index with Two Cladding Modes

By introducing Eq. (4), (9), and (11) with an LPFG sensor fully submerged in water (n_0 = 1.33) as a reference point, Eq. (3) can be further simplified into:

$$d\lambda_{res,m} = \lambda_{res,m}\Big|_{1.33,L}\left[dn_s \cdot K_{n_s,m}\Big|_{1.33,L} + dL_{liquid} \cdot K_{L_{liquid},m}\Big|_{1.33,L} + dn_s dL_{liquid} \cdot (K_{n_s,m}\Big|_{1.33,L} K_{L_{liquid},m}\Big|_{1.33,L} + \frac{\partial K_{L_{liquid},m}}{\partial n_s}\Big|_{1.33,L})\right] \tag{12}$$

Given the calibration coefficients for various sensitivity terms, the changes in liquid level and refractive index can be simultaneously evaluated by monitoring the wavelength shifts of two cladding modes of an LPFG sensor, LP_{0i} and LP_{0j}. In this study, the cladding modes LP_{06} and LP_{07} were selected for their significant power within the wavelength range of a commonly used broadband light source. In fact, both cladding modes were visible over a 400 nm wavelength range.

3. SENSOR DEVICE DESIGN

3. 1 Sensor Structure

As temperature and pressure induced strains increase in measurement environment, their effect must be taken into account in Eqs. (2) and (3). In particular, LPFGs are highly sensitive to temperature changes. A small variation of temperature environment may significantly affect the measurement accuracy for liquid level and surrounding RI. To compensate for environmental effects, a sensor device is proposed as schematically as shown in Figure 1a and it consists of two parallel LPFGs and one glass tube. One LPFG is installed outside the glass tube with two ends bonded on the glass tube, which is referred to as Out-LPFG, and the other LPFG is installed inside the glass tube with two ends of the glass tube sealed, which is referred to as In-LPFG. The Out-LPFG is the major sensing component for a simultaneous

measurement of liquid level and surrounding RI. The In-LPFG is applied to compensate for temperature and pressure effects on the device.

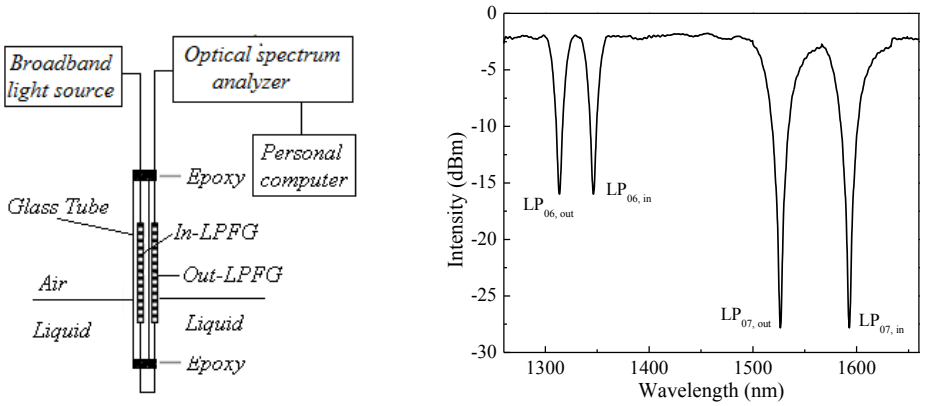

(a) Sensor structure (b) Typical sensor transmission spectrum

Fig. 1 Schematic view of sensor structure

As shown in Figure 1a, light coming from a broadband source sequentially travels through the two parallel LPFGs whose transmission spectrum is monitored with an optical spectrum analyzer (OSA) and analyzed by the connected personal computer. Figure 1b shows a typical transmission spectrum of the sensor device by using a 400 nm broadband light source. The two cladding modes of the In-LPFG (illustrated as $LP_{06,\,in}$ and $LP_{07,\,in}$ in Figure 1b) are used to simultaneously measure strain and temperature following the published procedure [33]. The two cladding modes of the Out-LPFG (illustrated as $LP_{06,\,out}$ and $LP_{07,\,out}$ in Figure 1b) are used to monitor liquid level and surrounding RI as well as environmental effects (temperature and pressure). A MATLAB program is developed with the personal computer to automatically remove environmental effects (temperature and pressure induced strains) on the device measurement by subtracting the resonant wavelength change of the In-LPFG from that of the Out-LPFG.

3.2 LPFG Parametric Analysis

For a more accurate measurement, several significant parameters are further studied in this paper including the selection of cladding modes, initial resonant wavelengths, and the fabrication process control.

1) Selection of cladding modes: As mentioned in Section 2, when the highest cladding mode of the CO_2-laser induced LPFG is less than 10^{th} order [30], the LPFG has negative sensitivity coefficients both for surrounding RI and liquid level, whose value increases with the order of cladding modes [29]. The negative sensitivity of the liquid level and environmental RI effect results in a downshifting resonant wavelength. The effects of increased RI and liquid level sensitivities are two fold because they increase the measurement nonlinearity and decrease the environmental stability of a sensor device [29]. Thus, the CO_2-laser induced LPFG with cladding modes of 8^{th} or higher order shows an extremely high RI sensitivity with high nonlinearity and low stability. For a more accurate piecewise linear approximation for RI detection, an LPFG with cladding mode lower than 8^{th} order is recommended.

On the other hand, the CO_2-laser induced LPFG has positive temperature sensitivity for cladding modes lower than 8^{th} order, which increases with the order of cladding modes [33]. The positive sensitivity results in an upshifting resonant wavelength. The CO_2-laser induced LPFG has negative strain sensitivity for cladding modes of 5^{th} or lower order and positive strain sensitivity for cladding modes of higher than 5^{th} order. The strain sensitivity is two orders of magnitude less than that of the temperature [33].

The characteristics of the CO_2-laser induced LPFG with negative liquid level and RI sensitivities versus positive temperature and strain sensitivities can benefit the design of a sensor device in that it enables a more accurate identification of parameters after the initial resonant wavelength of each mode has been reasonably selected. Therefore, to achieve an effective sensor device for simultaneous liquid level and surrounding RI detection, cladding modes LP_{06} and LP_{07} are selected for both In and Out-LPFG of the sensor device.

2) Initial resonant wavelengths (in air) and coupling between cladding modes: With two sequential in-line LPFGs, a strong mode coupling effect is expected between the two adjacent resonant wavelengths, which could lead to erroneous results if not properly taken into account. Thus, the initial resonant wavelengths of various cladding modes used in the proposed sensor device must be carefully selected for accurate measurements. To minimize or eliminate the coupling effect, it is recommended that the two

adjacent resonant wavelengths be set apart for an at least full width of the spectral resonance ($2\lambda_{FWHM,m}$) and the initial resonant wavelength of one cladding mode of the In-LPFG be larger than that of corresponding cladding mode of the Out-LPFG. For most CO_2-laser induced LPFGs, $\lambda_{FWHM,m}$ ranges from 25 nm to 30 nm. With a dynamic range of $2\lambda_{FWHM,m}$, the coupling effect is minimized [2] and the individual peaks of adjacent resonant wavelengths can be easily distinguished. With In-LPFG's resonant wavelengths longer than their corresponding values of the Out-LPFG as indicated in Figure 1b, the resonant wavelengths of various cladding modes would shift apart from each other as liquid level, liquid RI, temperature, and strain increase, facilitating the detection of multiple parameters.

3) LPFG fabrication process control: Used in both numerical and experimental simulations is the Corning SMF28e single mode fiber with a core diameter of 8.2 μm and cladding diameter of 125 μm. To obtain the designed initial resonant wavelengths of the sensor device, the LPFG fabrication process must be carefully controlled. The initial resonant wavelengths of the Out-LPFG can be estimated based on the application limit, e.g. dynamic range of the liquid RIs. The period of the Out-LPFG (Λ_{out}) is then determined accordingly using Eq. (1). With the period of the Out-LPFG determined, the fabrication period of the In-LPFG (Λ_{in}) can then be estimated by:

$$\Lambda_{In} = \Lambda_{out} + \Delta\Lambda \quad and \quad \Delta\Lambda = \frac{2\lambda_{FWHM,m}}{\Delta n_{eff,m,air}} \tag{13}$$

where $\Delta\Lambda$ represents the difference in grating period between Out- and In- LPFG.

The intensity of an LPFG sensor highly depends on the laser power and the radiation points on the fiber in addition to grating period. To achieve a specific intensity of the grating (>-20dB), 80~90 points of the laser radiation were used in sensor fabrication, resulting in a determined grating length L. In this study, LPFG sensors were fabricated by carefully following the published procedure that has been used for other fabrication parameter control [24]. The grating length was clearly marked during the fabrication process to ensure effective experimental validation tests.

4. EXPERIMENTS AND DISCUSSION

4.1 Test Setup and Procedure

Figures 2a and 2b respectively show a schematic view and a photo of the experimental setup for liquid level detection. Three sensor device prototypes were fabricated and tested by placing each of them along the centerline of a scaled plastic tube that was vertically fixed on a holder. For liquid level testing, the liquid was gradually poured at an interval of 1 mm into a plastic tube to simulate an actual change of liquid level.

The In-LPFG was connected to a broadband light source (BLS: Agilent 83437A with 400 nm light spectrum) and the Out-LPFG was connected to an optical spectrum analyzer (OSA: AQ6319 produced by YOKOGAWA). The wavelength monitored in this study ranged from 1260 nm to 1660 nm. All the In-LPFG was fabricated using 80 points of CO_2 laser radiation with a period of 0.375 mm, which amounts to a sensor length of approximately L=30 mm; and all the Out-LPFG was fabricated using 88 points of CO_2 laser radiation with a period of 0.363 mm, which amounts to a sensor length of approximately L=32 mm. Figure 1b shows a typical transmission spectrum of the LPFG sensor in air. The fabricated In-LPFG sensor had two cladding modes in the 400 nm wavelength range of interest, $LP_{06,\,in}$ at 1343 nm and $LP_{07,\,in}$ at 1568 nm. Similarly, the Out-LPFG had the two same cladding modes but with 1314 nm and 1515 nm wavelengths, respectively. Three sensor prototypes were fabricated and tested for various sensor characteristic validations.

In the following sections, individual detection of surrounding RI and liquid level, cross sensitivity between liquid level and surrounding RI, environmental effects, and simultaneous detection of both liquid level and RI are reported and discussed.

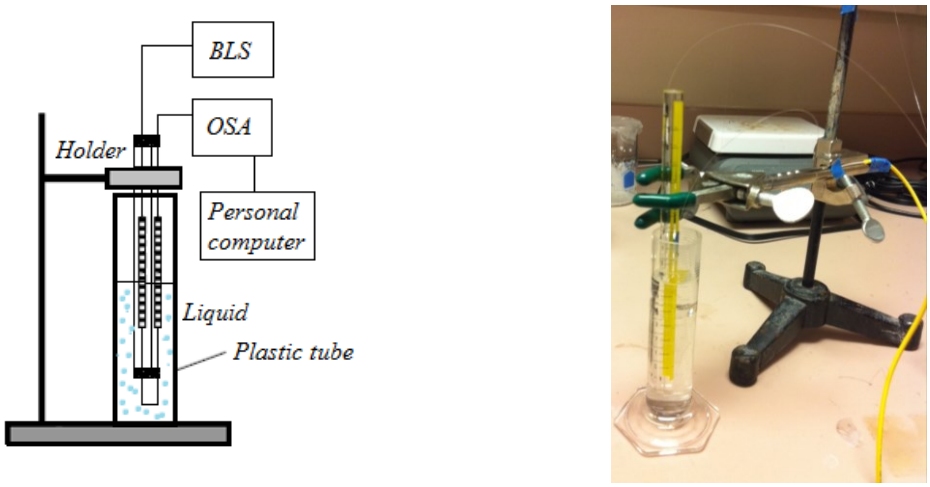

(a) Test setup (b) Photo of test setup

Fig. 2 Test setup

4.2 Surrounding Refractive Index Detection

The spectrum changes of the Out-LPFG with a surrounding RI of 1.33 to 1.44 were firstly simulated for cladding modes $LP_{06,\,out}$ and $LP_{07,\,out}$ following the procedure in [26, 28]. The filled squares and circles in Figure 3 represent the changes in simulated resonant wavelength of $LP_{06,\,out}$ and $LP_{07,\,out}$ according to Eqs. (4) and (5). Their relation with the surrounding RI is nonlinear, particularly towards a large index value. To simplify the simultaneous detection for multiple parameters, $K_{n,m}$ was approximated to a piecewise linear function of the surrounding RI in various ranges as defined in Table 1. The linear coefficients of various segments or the slopes of $K_{n,m}$-index curves are also presented in Table 1. For all segments, the R^2 value exceeds 0.93, indicating a good linear approximation of each nonlinear segment. To verify the simulated results, tests with the three fabricated sensor prototypes were conducted at constant temperature and surrounding pressure by completely immersing them in various types of liquids for surrounding RI detection. In this case, the spectrum of the Out-LPFG only will potentially change due to the variation of surrounding RIs. The liquids used in these tests included water (n_s=*1.33*), acetone (n_s=*1.36*), decane (n_s=*1.42*), and propylene glycol (n_s=*1.43*). The unfilled squares and circles in Figure 3 represent the resonant wavelength changes measured from the three LPFG sensor devices for cladding modes $LP_{06,\,out}$ and $LP_{07,\,out}$, respectively. The upper and lower bounds of each measured RI using three sensors are also presented in Figure 3. It can be seen from Figure 3 that the simulated results are in good

agreement with the experimental data. The slight difference between them is attributed to the potential variation of concentration in the tested liquid that directly affects the refractive index or to the high-order term in the Taylor expansion.

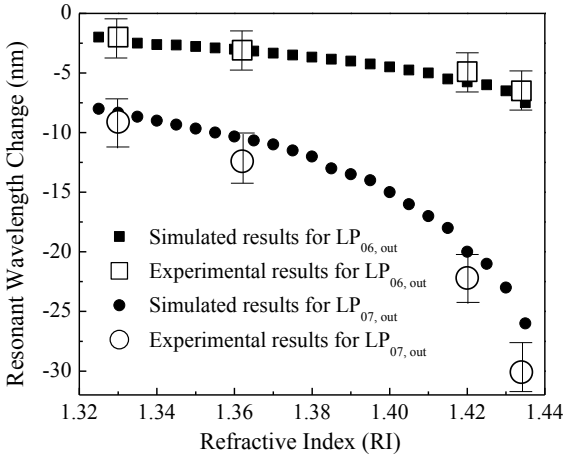

Fig. 3 Experimental and simulated resonant wavelength changes in various types of liquids

Table 1 Sensor sensitivity to refractive index in various ranges

Refractive index range	Cladding mode LP_{06}		Cladding mode LP_{07}	
	Slope of $K_{n,m}$-index	R^2	Slope of $K_{n,m}$-index	R^2
1.33 to 1.36	-26.43	0.94	-66.64	0.99
1.36 to 1.39	-33.26	0.99	-118.4	0.97
1.39 to 1.42	-61.43	0.98	-228.6	0.97
1.42 to 1.44	-150.0	0.93	-500.0	0.97

4.3 Liquid Level Detection

The spectrum changes of the Out-LPFG with water level (n_s = *1.33*) were simulated for cladding modes $LP_{06, out}$ and $LP_{07, out}$ following the procedure in [26, 28]. The filled squares and circles in Figure 4b represent the corresponding simulated resonant wavelength changes according to Eqs. (9) and (10). To verify the simulated results, tests with the three sensor prototypes were conducted at constant temperature and surrounding pressure by adding water at an interval of 1mm into the plastic tube as shown in Figures 2a and 2b.

Figure 4a shows spectrum changes of the Out-LPFG as water level increases. Figure 4b compares the experimental resonant wavelength changes with their corresponding simulations for a water level from 0

to 32 mm (full length of the grating). The unfilled squares and circles in Figure 4b represent the experimental resonant wavelength changes of the $LP_{06,\,out}$ and $LP_{07,\,out}$ modes, respectively. The upper and lower bounds of each measured water level using three sensors are also given in Figure 4b. It can be observed from Figure 4b that the experimental and simulated results follow the same trends for both cladding modes. The difference between the experiments and simulations likely resulted from the uneven water level rise during the tests. Overall, the water level sensitivity of the grating based on the regression analysis of the test data between 5 mm and 27 mm is -0.08 for $LP_{06,\,out}$ and -0.38 for $LP_{07,\,out}$.

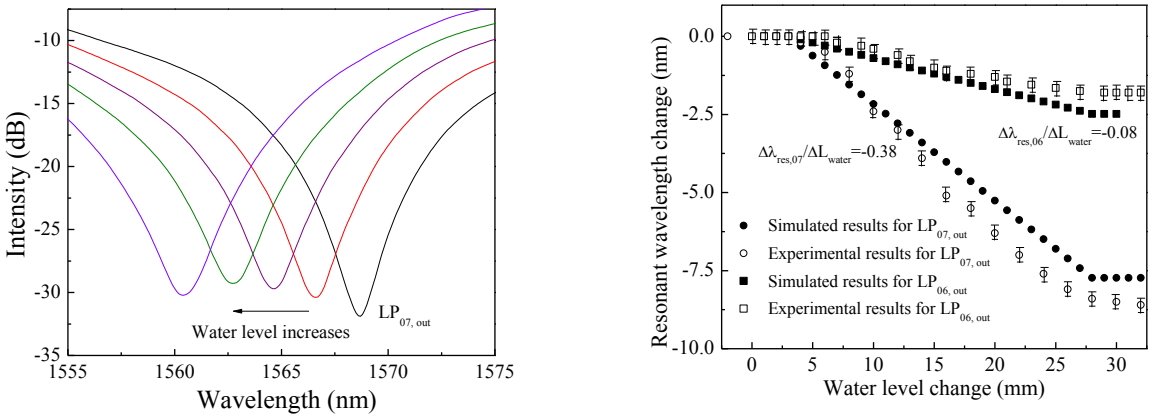

(a) Transmission spectrum change with water level (b) Experimental and simulated results

Fig. 4 Liquid level effect on transmission spectrum and sensor water level sensitivity

4.4 Cross Sensitivity

To investigate the cross sensitivity of the Out-LPFG for simultaneous liquid level and surrounding RI detection, another set of tests with the three sensor prototypes was conducted by taking into account the changes of both liquid level and surrounding RI at the same time under constant temperature and pressure. To this end, the 0wt.% to 40wt.% sugar solution at 10wt.% intervals was used. The refractive indices of five types of the sugar solution are 1.33, 1.35, 1.36, 1.38, and 1.40, respectively [31]. For each sugar solution, the liquid level was changed from 0 mm to complete immersion by following the test setup and procedure discussed in Section 4.1. Figures 5a and 5b show the resonant wavelength changes of one Out-LPFG with cladding modes $LP_{06,\,out}$ and $LP_{07,\,out}$, respectively. As the liquid level rose from the bottom to top across the gratings, the resonant wavelengths of the LPFG sensor first remained nearly

constant at low liquid level, then decreased almost linearly, and finally approached to an asymptotic value at high liquid level.

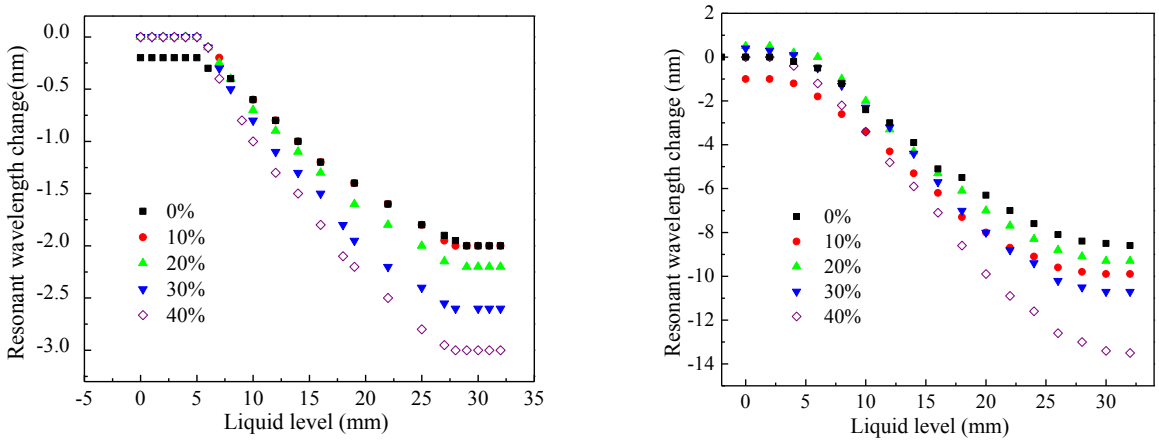

(a) Cladding mode $LP_{06, out}$ (b) Cladding mode $LP_{07, out}$

Fig. 5 Variations of resonant wavelengths with the level of water solution with different sugar concentration (% by weight)

According to Eq. (11), the simulated results for cross sensitivity are -0.74 nm/mm for $LP_{06, out}$ and -2.76 nm/mm for $LP_{07, out}$. The experimental results are presented in Figure 6 for the liquid level sensitivities of the gratings in various sugar solutions and their regression to straight lines. The R^2 values for both cladding modes $LP_{06, out}$ and $LP_{07, out}$ exceed 0.96, indicating a satisfactory linear regression. Table 2 summarizes the average water level sensitivity of the tested Out-LPFG and the cross sensitivity with water as a reference. For a refractive index range of 1.34 to 1.40, the average slopes of the straight lines or the cross sensitivities of the gratings are -0.78 and -2.86 for $LP_{06, out}$ and $LP_{07, out}$, respectively. The experimental results differ from their corresponding simulations by less than 5%. For refractive indices outside the range, the cross sensitivities can still be used for an approximate prediction of the liquid level and surrounding RI.

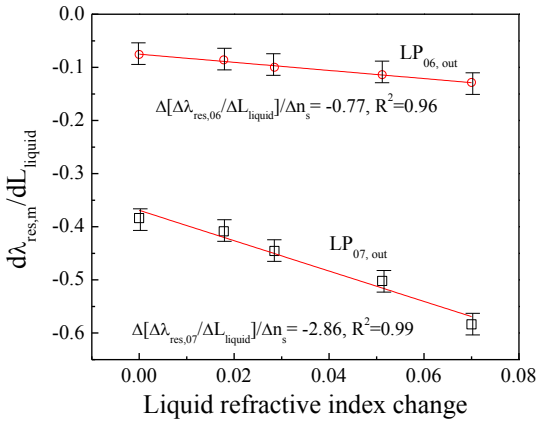

Fig. 6 Cross sensitivity of $LP_{07,\ out}$ and $LP_{06,\ out}$ of the Out-LPFG sensor

Table 2 Calibrated water level sensitivity and the cross sensitivity

Cladding mode	$K_{L_{liquid},m}$ (nm/mm)	$\frac{\Delta\left(\frac{\Delta\lambda_{res,m}}{\Delta L_{liquid}}\right)}{\Delta n_s}$ (nm/mm)
$LP_{06,\ out}$	-0.08	-0.77
$LP_{07,\ out}$	-0.39	-2.86

4.5 Environmental effects

To validate the effectiveness of the In-LPFG environmental compensation to other measurements by the Out-LPFG, the three sensor prototypes were tested for various changes of temperature and strain (representing the effect of pressure). The temperature tests were conducted in a controlled temperature chamber with no changes in liquid level, RI, and surrounding pressure. The temperature was increased from 22 °C (room temperature) to 300 °C at an interval of 25 °C. Figures 7a and 7b show the experimental wavelength changes of the In-LPFG and Out-LPFG in cladding mode LP_{07} and LP_{06}, respectively. It can be clearly seen that the variation among the three sensor devices at specific temperatures is insignificant. The In-LPFG and Out-LPFG of the sensor devices have almost the same temperature sensitivity of 0.163 nm/°C for LP_{07} and 0.098 nm/°C for LP_{06}, validating the effectiveness of using the In-LPFG for temperature compensation of the Out-LPFG.

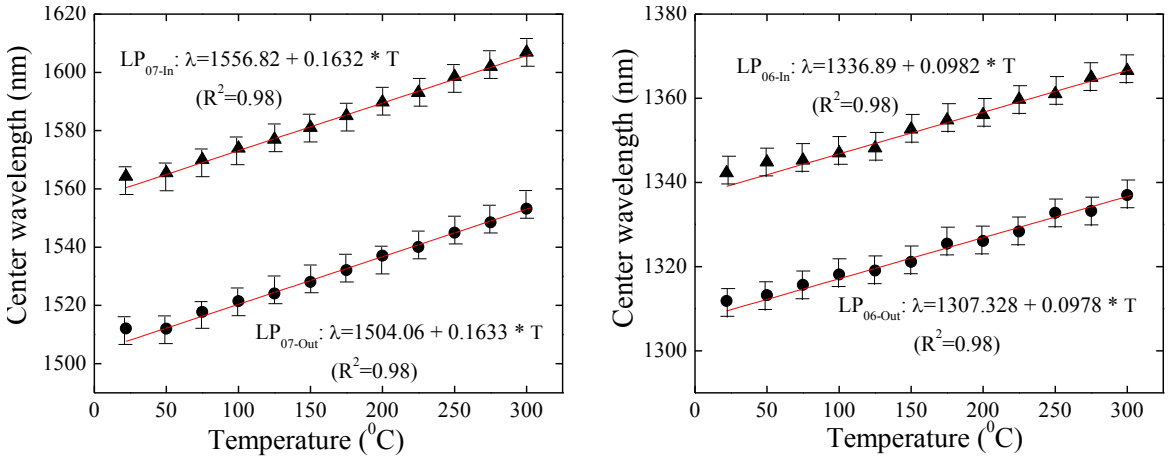

(a) Temperature sensitivity for LP_{07} (b) Temperature sensitivity for LP_{06}

Fig. 7 Temperature sensitivity of two the sensor device's LPFGs

To validate the pressure compensation of the proposed sensor device, strains were applied to the sensor device to simulate the pressure effect. One end of the three sensor prototypes were bonded on an automatic controlled movable stage and the other end of the sensor prototypes were bonded on a fixed stage. The moving of the automatic controlled movable stage would strain the sensor devices that would simulate the pressure induced strain on the sensors. The strain tests were performed in air without changes in liquid level, RI, and temperature environment. The strain was increased from 0 to 2,000 με with an interval of 250 με throughout the tests. Figures 8a and 8b show the cladding mode LP_{07} and LP_{06} wavelength changes of the In-LPFG and Out-LPFG in the three sensor devices under various strains. It can be observed from Figure 8 that the variation among three sensor devices is small and the In-LPFG and Out-LPFG of the sensor devices have almost the same strain sensitivity. These test results validate the effectiveness of using the In-LPFG for pressure induced strain compensation of the Out-LPFG. Indeed, the strain sensitivity of both LPFGs is approximately 4.5×10^{-4} nm/με for LP_{07} and 4.0×10^{-4} nm/με for LP_{06}.

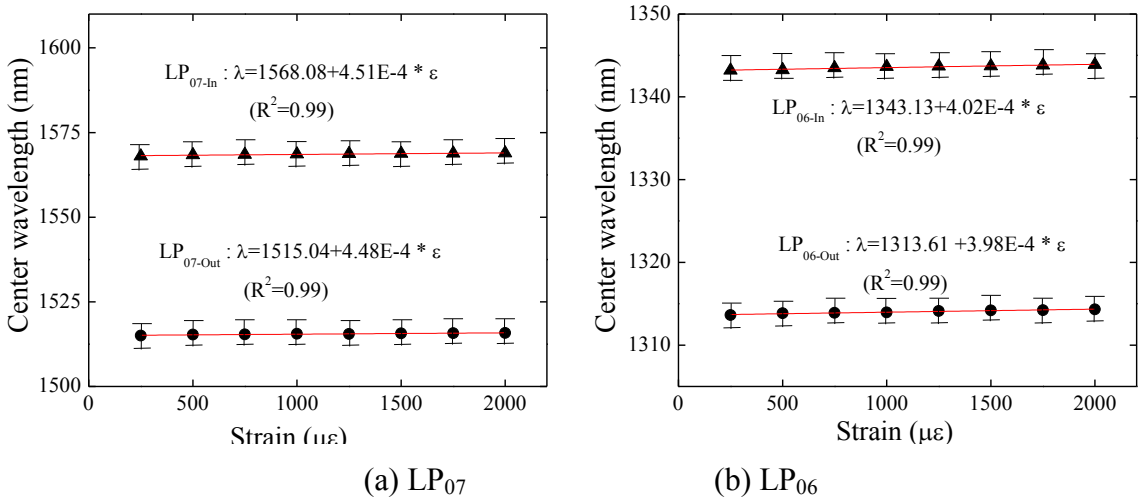

Fig. 8 Strain sensitivity of In-LPFG and Out-LPFG in the proposed sensor device

4.6 Simultaneous Liquid Level and Refractive Index Detection

To validate the capability of the developed sensor device for simultaneous liquid level and RI detection using Eq. (12), 18 tests were performed using the three sensor prototypes in propylene glycol with $n_s = 1.43$ and another 16 tests in decane with $n_s = 1.42$ for level increasing and decreasing for three times. Figures 9a and 9b show the experimental RIs and liquid levels determined by Eq. (12) using the Out-LPFG only and the entire sensor device (Out-LPFG and In-LPFG), respectively. The actual liquid level, represented by the black line in Figure 9, was directly read from a scaled plastic tube with a minimum mark of 1 mm. Therefore, the liquid level resolution is claimed to be within 1 mm though it is theoretically related to the grating period, Λ. The coefficient of variation of the experimental RI data is 10% without the In-LPFG and is reduced to less than 5% with the environmental compensation by the In-LPFG, proving the effectiveness of environmental compensation strategy in the proposed sensor device. In addition, a good repeatability of the test data (5% only with the environmental compensation) has been achieved. Figure 9 also shows that the experimental RI is within ±0.005 around the actual RI when the Out-LPFG only was used. With the compensation from the In-LPFG, the maximum difference between the experimental and actual RIs is reduced to be within ±0.002 or 5% of the actual value. The 5% variance in RI is likely attributed to such factors as the resolution of the grating output recording, the

variance of the liquid refractive index to the reference data, and the high-order terms in the Taylor expansion.

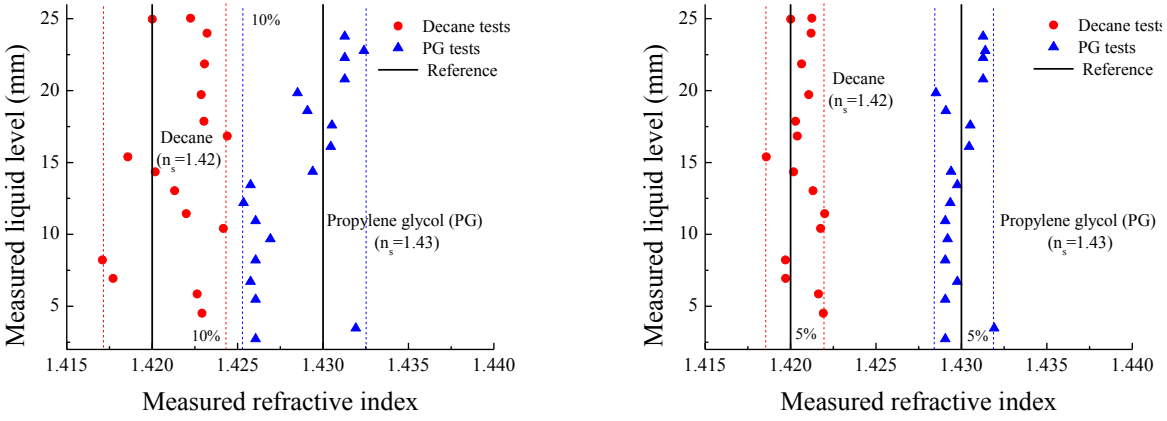

(a) Test results with Out-LPFG only (b) Test results with In-LPFG and Out-LPFG

Fig. 9 Simultaneous liquid level and refractive index detection

5. CONCLUSIONS

In this paper, a fiber optic sensor device based on LPFGs was proposed for simultaneous detection of liquid level and liquid refractive index by monitoring the resonant wavelength changes of two cladding modes. The sensor device consists of two LPFGs: one placed inside a glass tube for environmental compensation and the other outside the glass tube for liquid level and surrounding RI measurements. In this study, cladding modes, LP_{06} and LP_{07}, were selected for each LPFG. For each cladding mode of the Out-LPFG, a Taylor expansion of the resonant wavelength shift as a function of the changes in liquid level and surrounding RI was proposed and approximated by the first three terms. These terms were analytically characterized for the sensor's sensitivities to liquid level, surrounding RI, and their cross effect. Specifically, the change in resonant wavelength of the LPFG sensor varied almost linearly with the change in liquid level and nonlinearly with the change in surrounding RI. To facilitate a simultaneous evaluation of liquid level and surrounding RI, a piecewise linear approximation of the nonlinear relation was introduced. The proposed LPFG sensor, analytical sensitivity coefficients, environmental effects, and the evaluation algorithm for liquid level and RI were validated experimentally. The analytically derived

cross sensitivity coefficient was found to differ from test data by less than 5% and 10% with and without the implementation of the In-LPFG, respectively. The predicted liquid level and RI by the proposed algorithm were in good agreement with their actual values with the maximum difference of ±1 mm for liquid level and ±0.005 for surrounding RI based on experiments. The developed sensor device can be potentially used in many applications such as water resources, environmental engineering, flood monitoring, and chemical processing and storage.

REFERENCES

[1] Vengsarkar A M, Pedrazzani J R, Judkins J B, Lemaire P J,Bergano N S, and Davidson C B 1996 Long-period fiber grating based gain equalizers *Opt Lett* **21** 336-338

[2] Vengsarkar A M, Lemaire P J, Judkins J B, Bhatia V, Erdogan T, and Sipe J E 1996 Long-period fibre gratings as band rejection filters *J Lightwave Technol* **14** 58-65

[3] Bhatia V 1996 Optical fiber long-period grating sensors *Optic Letters* **21(9)** 692-469

[4] Lee B H,Liu Y, Lee S B, Choi S S, and Jang J N 1997 Displacements of the resonant peaks of a long-period fiber grating induced by a change of ambient refractive index *Opt Lett* **22** 1769-1771

[5] Patrick H J, Kersey A D, and Bucholtz F 1998 Analysis of the response of long period fiber gratings to external index of refraction *J Lightwave Technol* **16** 1606-1612

[6] Chong J H, Shum P, Haryono H, Yohana A, Rao M K, Lu C, and Zhu Y 2004 Measurements of refractive index sensitivity using long-period grating refractometer *Opt Commun* **229** 65-69

[7] Duhem O, Henninot J F, Warenghem M, and Douay M 1998 Demonstration of long- period-grating efficient couplings with an external medium of a refractive index higher than that of silica *Appl Opt* **37** 308-310

[8] Libish T M, Bobby M C, Linesh J, Nampoori V P N, and Radhakrishnan P 2012 Experimental analysis on the response of long period grating to refractive indices higher and lower than that of fiber cladding *Microwave and Optical Technol. Letters* **54 (10)** 2356-2360

[9] Zhou X J, Shi S H, Zhang Z Y, and Liu Y 2012 Refractive index sensing by using mechanically induced long-period grating *IEEE Photonics Journal* **4(2)** 119-125

[10] Xuan H, Jin W, and Zhang M 2009 CO_2 laser induced long period gratings in optical microfibers *Opt Express* **7(24)** 21882-90

[11] Li B Y, Jiang L, Wang S M, Tsai H L, and Xiao H 2011 Femtosecond laser fabrication of long period fiber gratings and applications in refractive index sensing *Optics & Laser Technology* **43** 1420-1423

[12] Wang K and Pickrell G 2011 Long period gratings in random hole optical fibers for refractive index sensing *Sensors* **11 (2)** 1558-1564

[13] Flores-Llamas I F, Kolokoltsev O, and Svyryd V 2006 Refractometric sensors based on long period optical fiber gratings *Rev. Mex. Fís.* **S52** 75-78

[14] Flores-Llamas I, Svyryd V, and Khotiaintsev S N 2008 Design of long-period fiber grating refractometric sensors with linear response by a genetic algorithm *IEEE Sensors Journal* **8(7)** 1130-1137

[15] Falciai R, Mignani A, and Vannini A 2001 Long period gratings as solution concentration sensors *Sensors and Actuators B: Chemical* **74(1-3)** 74-77

[16] Wang J N 2011 A microfluidic long-period fiber grating sensor platform for Chloride ion concentration measurement *Sensors* **11(9)** 8550-8568

[17] Khaliq S, James S W, and Tatam R P 2001 Fiber-optic liquid-level sensor using a long-period grating *Optic Letters* **26** 1224-1226

[18] Grice S, Zhang W, Sugden K, and Bennion I 2009 Liquid level sensor utilizing a long period fiber grating *Proceedings of SPIE* **7212** 72120C-1

[19] Mao B and B Zhou 2012 Liquid level measurement sensor using a long period fiber grating *Proceedings of SPIE*, **8351**, 1N (6pages)

[20] Fu H Y, Shu X W, Zhang A, Liu W S, Zhang L, He S L, and Bennion I 2011 Implementation and characterization of liquid-level sensor based on a long-period fiber grating Mach–Zehnder interferometer *IEEE Sensors Journal* **11(11)** 2878-82

[21] Wang J N and Luo C Y 2012 Long-period fiber grating sensors for the measurement of liquid level and fluid-flow velocity *Sensors* **12** 4578-4593

[22] Jiang Q, Hu D, and Yang M 2011 Simultaneous measurement of liquid level and surrounding refractive index using tilted fiber Bragg grating *Sensors and Actuators A: Physics* **170(1-2)** 62-65

[23] Selleri S, Poli F, Foroni M, and Cucinotta A 2007 Simultaneous liquid level and refractive index measurements with a POF-based sensor *Proceedings of SPIE* **6585** 65851F

[24] Li Y J, Wei T, Montoya J A, Saini S V, Lan X W, Tang X L, Dong J H and Xiao H 2008 Measurement of CO2-laser-irradiation-induced refractive index modulation in single-mode fiber toward long-period fiber grating design and fabrication *Applied Optics* **47(29)** 5296-5304

[25] Hill O, Malo B, Vineberg K, Bilodeau F, Johnson D 1990 Efficient mode conversion in telecommunication fiber using externally written gratings *Electronics Letters* **26** 1270-1272

[26] Farahi F 1990 Simultaneous measurement of temperature and strain: cross-sensitivity considerations, *Journal of Lightwave Technology* **8(2)** 138-142

[27] Morse P M and Feshbach H 1953 Derivatives of analytic functions, Taylor and Laurent Series §4.3 in Methods of Theoretical Physics, Part I. New York: McGraw-Hill, pp. 374-398

[28] Odibat Z M and Shawagfeh N T 2007 Generalized Taylor's formula *Applied Mathematics and Computation* **186** 286-293

[29] Shu X W, Zhang L, and Bennion I 2002 Sensitivity characteristics of long-period fiber gratings *Journal of Light-wave Technology* **20(2)** 255-266

[30] Lan X W, Han Q, Huang J, Wang H Z, Gao Z, Kaur A, and Xiao H 2013 Turn-around point long-period fiber grating fabricated by CO_2 laser for refractive index sensing *Sensors and Actuators B: Chemical* **177** 1149-1155

[31] James S W and Tatam R P 2003 Optical fibre long-period grating sensors: characteristics and application *Meas. Sci. Technol.* **14** R49

[32] Hamann B and Chen J L 1994 Data point selection for piecewise linear curve approximation *Computer Aided Geometric Design* **11(3)** 289-301

[33] Huang Y, Zhou Z, Zhang Y N, Chen G, and Xiao H 2010 A Temperature self-compensated LPFG sensor for large strain measurements at high temperature *IEEE Transactions on Instrumentation and Measurements* **59(11)** 2997-3004

[34] Bhatia V, Campbell D K, Sherr D, D'Alberto T G, Zabaronick N A, Ten Eyck G A, Murphy K A, and Claus R O 1997 Temperature-insensitive and strain-insensitive long-period grating sensors for smart structures *Optical Engineering* **36** 1872

[35] Yunus W M and Rahman A A 1988 Refractive index of solutions at high concentrations *Applied Optics* **27(16)** 3314-43